Microbial Pathogenesis 123 (2018) 410–418

Contents lists available at ScienceDirect

Microbial Pathogenesis

journal homepage: www.elsevier.com/locate/micpath

Study of *Helicobacter pylori* infection on lung using an animal model

A.C. Arismendi Sosa[a,*], A.G. Salinas Ibáñez[a], M.V. Pérez Chaca[b], A.B. Penissi[c], N.N. Gómez[b], A.E. Vega[a]

[a] Área Microbiología, Facultad de Química, Bioquímica y Farmacia, Universidad Nacional de San Luis, San Luis, Argentina
[b] Área de Morfología, Facultad de Química, Bioquímica y Farmacia, Universidad Nacional de San Luis, San Luis, Argentina
[c] Instituto de Histología y Embriología "Dr. Mario H. Burgos" (IHEM-CONICET), Facultad de Ciencias Médicas, Universidad Nacional de Cuyo, Mendoza, Argentina

ABSTRACT

Helicobacter pylori infection has been reported to be associated with extra-digestive disorders such as respiratory diseases; however, the impact of *H. pylori* on lung is incompletely understood. Inflammatory response is mediated by the release of cytokines, interferon, and enzymes such as metalloproteinases (MMPs). This may contribute to collagen accumulation during the early phase of infection. MMP expression is an important factor for the proliferation and infiltration of lung cells in the process of fibrosis formation. The aim of this work was to study the impact of the infection with *H. pylori* on lung using a mouse model. We looked for histological lesions of lung infected with the microorganism as well as the expression of inflammatory and of endothelial dysfunction markers. C57BL/6 wild type (WT) mice were infected by orotracheal instillation with 20 μl of 1×10^8 *H. pylori* reference strain suspension once per day for 3 days. Animals infected and controls were sacrificed at 3, 7, 14, 21 and 30 days. The lung from mice were stained with Hematoxylin-Eosin (H-E), Masson's Trichromic and Periodic Acid Schifft (PAS) for histological study. Also, lipid hydroperoxides and enzime catalase (CAT) activity were determined. Expression level of multiple markers implicated in inflammation (tumor necrosis factor (TNF)-α, interleukin (IL)-1β, IL-4, IL-6, IL-8, IL-10; metalloproteinase MMP-9) and markers of endothelial dysfunction (I-CAM and V-CAM) was determined from lung tissues mRNA using RT-PCR. Results showed that *H. pylori* induced morphological changes in the lung tissue with recruitment of inflammatory cells and lung parenchymal cell degradation. The mRNA of IL-1β and TNF-α; MMP-9, I-CAM and V-CAM increased at 3–7 days infections. Also, iNOS, IL-8 and Phosphocholine cytidyltransferase (CCT) increased with lung injury. Anti-inflammatory interleukin as: IL-4, and IL-10 increased at 7 and 14 days post infection respectively. The results obtained suggest that the pathogenic mechanism of *H. pylori* on lung could be strongly associated with lung injury as indicate the expression increased of inflammatory mediators and markers of endothelial dysfunction.

1. Introduction

Respiratory tract diseases are among several extragastric diseases reported to be associated with *Helicobacter pylori* infection.

H. pylori is a Gram-negative bacteria that selectively colonization a hostile environment as stomach mucosa in greater than half of the global population. Infection leads chronic inflammation of the gastric mucosa increasing the risk of several upper gastrointestinal disorders such as gastritis, peptic ulcers, and gastric adenocarcinoma [1–3].

T-helper cells (Th) play a very important role in host defense against pathogens via different types of cytokine secretion. They are comprised of three subsets, Th1, Th2, and Th17 cells, which are defined by the cytokines that produce [4].

Cytokines that characterize the Th1 and Th17 mediated immune responses are interferon γ (IFN-γ), tumor necrosis factor α (TNF-α), and interleukin-1β (IL-1β), IL-6, IL-8 and IL-17 respectively. While Th2 related cytokines IL-4 and IL-10 are the most important regulatory cytokines, inhibiting cell mediated immune responses [5,6].

Shi et al. [7] demonstrated that IL-6 from activated macrophages/dendritic cells is required for Th17 cell differentiation in murine systems. Other studies showed that IL-17 synergizes with other cytokines such as TNF-α and IL-6 to enhance the inflammatory response. In this sense, studies on inflammatory process in patients with rheumatoid arthritis have reported that IL-17 acts in synergy with IL-1β and TNF-α [8]; [9]. Additionally, IL-17 stimulated gastric epithelial cells to produce metalloproteinases (MMPs). On the other hand, the main immune mechanism to detain inflammation is IL-10, which can suppress Th1, Th2, and Th17 immune responses [10].

H. pylori infection mainly induces a mixed T-helper, Th17/Th1, cells response that contributes to gastric inflammation and microorganism colonization [11]. Thus, the inflammatory response due to stimulation of the epithelial cells produce various proinflammatory cytokines and chemokines (including IL-8, IL-1β, IL-6, TNF-α), followed by recruitment of immune cells into the gastric mucosa. This cause changes in the normal morphology of gastric epithelial cells, by damage to DNA and induces synthesis of reactive oxygen species (ROS); which contribute to major impact in the final outcome of the infection [12]. The MMP such as MMP-9 expression contributes to tissue damage during *H. pylori*-

* Corresponding author. Área Microbiología, Facultad de Química, Bioquímica y Farmacia, Universidad Nacional de San Luis, Ejercito de los Andes 950, Bloque 1 piso 1, San Luis, Argentina.
E-mail address: acarismendi@gmail.com (A.C. Arismendi Sosa).

https://doi.org/10.1016/j.micpath.2018.07.038
Received 23 May 2018; Received in revised form 24 July 2018; Accepted 25 July 2018
Available online 26 July 2018

associated gastritis and may increase invasion of microorganism [13,14]. It has also been reported that MMP-9 enhances the host susceptibility to pulmonary infection with *Francisella tularensis* [14,15].

Several microorganisms may cause diseases from the primary site of infection by interfering with different biologic processes [16]. Is well known that lung and the cells that constitute the digestive system have the same embryological origin [17]. So, the persistent of *H. pylori* in the gastric epithelium, induce systemic effects and immune response that can cause lesion far away from the primary infection site. Moreover, both *H. pylori* infection and respiratory disease are characterized by the attraction of granulocytes as well as B- and T-cell mediated response [18]. On the other hand, *H. pylori* is present in the oral cavity, therefore it is not surprising that many studies have demonstrated the presence of microorganism in upper respiratory system mucosa. This increases the possibility that *H. pylori* has a potential role in the onset of diseases such as sinusitis, adenotonsillar hypertrophy, pharyngitis and laryngitis. Also, in the last years, a possible association between *H. pylori* and pulmonary disease has been suggested [19].

The hypotheses indicate that the role in extragastric disease of *H. pylori* could be through of mechanism such as the production of an inflammatory state, induction of molecular mimicry mechanism by expressing proteins that mimic host peptides [20] or aspiration into the lung of *H. pylori* products, such as toxins [21]. In the case of the respiratory system, patient that have gastroesophageal reflux, could facilitate the infection with *H. pylori* in the lung due to the gastric content may easily reach the airways. If this contains the bacteria, it might colonize the respiratory system through the ora-pharyngeal-laryngeal routes and trigger inflammation [18]. However, the impact on lung of *H. pylori* has not been investigated.

The aim of this work was to study the impact of the infection with *H. pylori* on lung using a mouse model. We looked for histological lesions of lung infected with the microorganism as well as the expression of inflammatory and of endothelial dysfunction markers.

2. Materials and methods

2.1. Animals and experiment protocol

C57BL/6 wild-type (WT) mice were used. They were keep under specific-pathogen-free condition at UNSL's bioterio, according protocol approved by the Comité Institucional de Cuidado y Uso de Animales (CICUA). The male mice of 6–12 weeks old, 25–30 g approximately, was provided with sterile food and water *ad libitum* during the experience. Three independent experiments were carried out with 4 mice per group (total n = 20 mice).

2.2. Bacteria and experimental protocol for H. pylori infection

Strain NCTC 11638 (kindly provided by Dra. Teresa Alarcón Cavero, Microbiology Service of Hospital Universitario de la Princesa, Madrid, Spain) was used for infection. *H. pylori* strain were grown in Mueller-Hinton agar (MHA) supplemented with 7% horse blood (MHA-HB) at 37 °C under microaerophilic conditions and identified by microscopy, urease, catalase and oxidase tests. A bacterial suspension of 1–5x10^8 colony forming units for millilitre (CFU/ml) was prepared for the infection. Mice were divided into two groups, infected and control. To the infected group, 50 µl of the microorganism suspension was administered by orotracheal instillation; while to the control group it was given phosphosaline buffer (PBS 1× pH 7.4) sterile.

2.3. Bacteriological determination and quantification of mucosal lesion

The *H. pylori* count in the lung, mesenteric lymph nodes (MLN) and stomach at 3, 7, 14, 21 and 30 days post-orotracheal infection, was performed by organs homogenization, obtained aseptically in saline solution, using an Ultra Turrax IKA® T18 basic teflon fabric homogenizer. Homogenates and dilutions thereof (100 µl) from both control and infected groups were plated on blood agar plates, and incubated at same conditions as previously described.

The molecular determination was performed by PCR assay using 16S rRNA primers. *H. pylori* DNA was obtained from lung in all days' post-infection. Primers sequence was: Forward: 5′-GGAGGATGAGGTT TTAGGATTG-3′ and Reverse: 5′-TCGTTTAGGGCGTGGACT-3'.

The number of lesions in the glandular part of the stomach was measured under an illuminated magnifying microscope. Long lesions were counted and their lengths were measured. Petechial lesions were counted, and then each five petechial lesions were taken as 1 mm of ulcer according to described by Ref. [22].

2.4. Bronchoalveolar lavage (BAL)

After 3, 7, 14, 21 and 30 days post-infection, mice from both groups were anesthetized with ketamine-xylazine and the trachea was cannulated. BAL was performed with PBS 1×, which was collected, centrifuged and supernatants were frozen at −20 °C for future analysis.

2.5. Characterization/typification of cell populations

To evaluate the cellular immune response, the first BAL (approximately 1 ml) was centrifuged and the supernatant fixed with methanol and stained with Giemsa. Total of 100 cell were counting and identified by the characteristic morphology using light microscopy.

2.6. Histopathological analysis of lungs

The lung from one mouse from each group and at each time point extracted aseptically was fixed with Bouin's liquid, and the paraffin wads were mounted. The obtained sections were stained with Hematoxylin-Eosin (H-E), Masson's Trichrome and Periodic Acid Schifft (PAS) and visualized under an Olympus BX50 optical microscope connected to a digital camera. The analysis of the microphotographs was performed with the ImageJ system. Histopathologic evidence for lung injury was analysed as previously described by Ref. [23]. Briefly, the lesion was scored on a scale from 0 (normal) to 10 (most severe) essentially as degree of vascular congestion, hemorrhagic edema, thickening of alveolar septum (edema), hyaline membrane formation in the distal airway, and neutrophil accumulation. A total score of less than 4 was considered a mild injury, a score of 4–8 was classified as moderate, and a score greater than 9 was classified as severe.

2.7. Determination of the gene expression

Total RNA from lung tissue was extracted using TRIzol (Life Technologies) and RNA quantification was performed by spectrophotometric measurement using a NanoDrop ND- 1000 (NanoDrop Technologies). RNA sample was adjusted to give a final concentration of 2 ng/µl. Synthesis of cDNA was performed using 2 µg of total RNA, Moloney Murine retrotranscriptase Leukemia virus reverse transcriptase (Invitrogen) and random primers. From the cDNA thus obtained, the genes coding for TNF-α, iNOS, IL-1β, IL-8, IL-17, IL-10, IL-4, MMP-9, CIT, I-CAM1, V-CAM1 and β-actine as housekeeping were amplified by PCR (Table 1). The fragments obtained were identified on agar gel stained with Gel Red (GenBiotech). The size of the DNA fragment was determined by comparison with the Molecular Weight marker, 6-band markers PCR with a PM range of 50–1000 bp. Differential analysis of gene expression was performed by semi-quantification of the bands with an image analyser (WCIF ImageJ). The ratio for a given gene respect to the constitutive gene and the expression ratio of that gene for a given time of infection to the control, were established. Values less than 1 correspond to a decrease in expression and values greater than 1 correspond to an increase in expression.

Table 1
Primers used for RT-PCR.

Target Genes	Orientation	Sequence (5′-3′)
B-actine	Forward	CTCTTTGATGTCACGCACGATTTC
	Reverse	GTGGGCCGCTCTAGGCAGCAA
TNF-α	Forward	ATGAGCACAGAAAGCATGATC
	Reverse	TACAGGCTTGTCACTCGAATT
iNOS	Forward	GAGAGATCCGATTTAGAGTCT
	Reverse	GAGAGATCCGATTTAGAGTCT
IL-1β	Forward	TGCAGAGTTCCCCAACTGGTACATC
	Reverse	GTGCTGCCTAATGTCCCCTTGAATC
IL-8	Forward	GTGCTGCCTAATGTCCCCTTGAATC
	Reverse	GTGCTGCCTAATGTCCCCTTGAATC
IL-4	Forward	GAATGTACCAGGAGCATATC
	Reverse	CTCAGTACTACGAGTAATCCA
IL-10	Forward	CTCAGTACTACGAGTAATCCA
	Reverse	AAGCGGCTGGGGGATGAC
I-CAM	Forward	TAAGAGGACTCGGTGGATGG
	Reverse	TTTCCCCAGACTGTCACAGG
V-CAM	Forward	TGACAAGTCCCCATCGTTGA
	Reverse	ACCTCGCGACGGCATAATT
CIT	Forward	AGGCTACTGTGACCGAGTA
	Reverse	AGTCACCCTGACATAGGGCT
MMP-9	Forward	GCATACTTGTACCGGTATGG
	Reverse	TGTGAGTTTATGATGGTCCC
IL-17	Forward	TCCAGAAGGCCCTCAGACTA
	Reverse	CTCGACCCTGAAAGTGAAGG

2.8. TBARS determination

Lung homogenates were used for thiobarbituric acid (TBA) assay, and the level of lipoperoxidation products, mainly malondialdehyde (MDA), were determined spectrophotometrically as thiobarbituric acid reactive substances (TBARS) [23]. OD was read at 535 nm and 575 nm to correct baseline absorption MDA equivalents were calculated using the difference in OD at the two wavelengths and quantification was made by using a calibration curve.

2.9. Catalase (CAT)

Activity was measured in lung homogenate. A reagent mixture containing 50 mM K-phosphate buffer (pH 6.5) and 3 mM H_2O_2 diluted with 50 mM phosphate buffer (pH 7) was used. Reaction was started by adding sample and the absorbance at 240 nm was monitored at room temperature. The decrease in absorbance was recorded and activity calculated using a molar extinction coefficient of 40 M^{-1} cm^{-1}.

2.10. Statistical analyses

Statistical differences were tested by analysis of variance (ANOVA) or by unpaired Student's test. All data are expressed as the mean ± S.E.M. (Standard Error of Mean). A probability of $p < 0.05$ was considered significant.

3. Results

3.1. Bacterial recovery

The recovery of *H. pylori* in lung tissue as well as in mesenteric lymph nodes (MLN) and stomach was determined by viable cell counts. The microorganism was identified by microscopy, urease, catalase and oxidase positive tests.

H. pylori was isolated from the lung at the 3 and 7 day post infection. The small and transparent colonies was Gram stained and the characteristic gram-negative helical shape of bacterium was observed (Fig. 1A and B). The viable count was $1.3 \times 10^4 \pm 1.5$ CFU/ml at 3 days post infection and bacterial load decreased $2.3 \times 10^3 \pm 1.8$ CFU/ml at 7 days post infection.

There was no recovery of the microorganism in MLN and stomach of mice infected by orotracheal route. However, the presence of lesions in gastric mucosa showed three compared to seven ulcers in control and infected mice respectively by 100 microscopic fields observed.

The detection of *H. pylori´s* DNA was performed by PCR. Intensity of bands amplified of 16 S rRNA gene was strong in the first period of infection (3 and 7 days), faint at 14 and 21 days and negative at 30 days post-infection (Fig. 1C).

3.2. Cell population typification

The analysis of the influx of different cells in the lung after infection was examined from the cellular populations present in BAL. The count

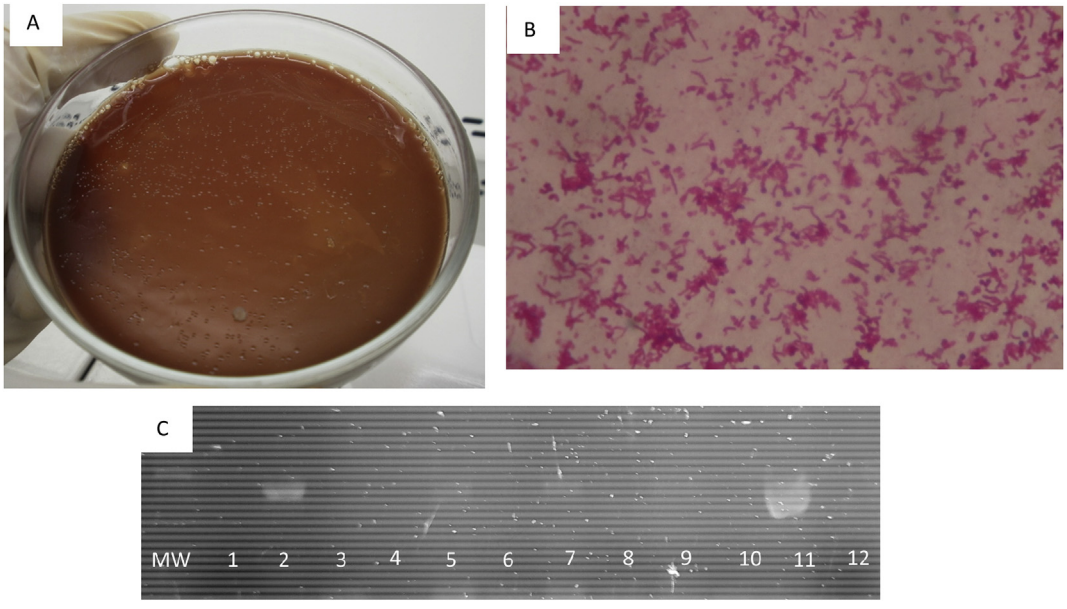

Fig. 1. A) Culture of *H. pylori* isolated from lung at 3 days after infection. **B)** Gram stain from *H. pylori* colonies. **C)** DNA 16S rRNA gene detection by PCR. MW: Molecular Weight, lane 1: Control 3 days, lane 2: Infection 3 days, lane 3: Control 7 days, lane 4: Infection 7 days, lane 5: Infection 7 days, lane 6: Control 14 days, lane 7: Infection 14 days, lane 8 control 21 days, lane 9: infection 21 days, lane 10: infection 30 days, lane 11: positive control, lane 12: negative control.

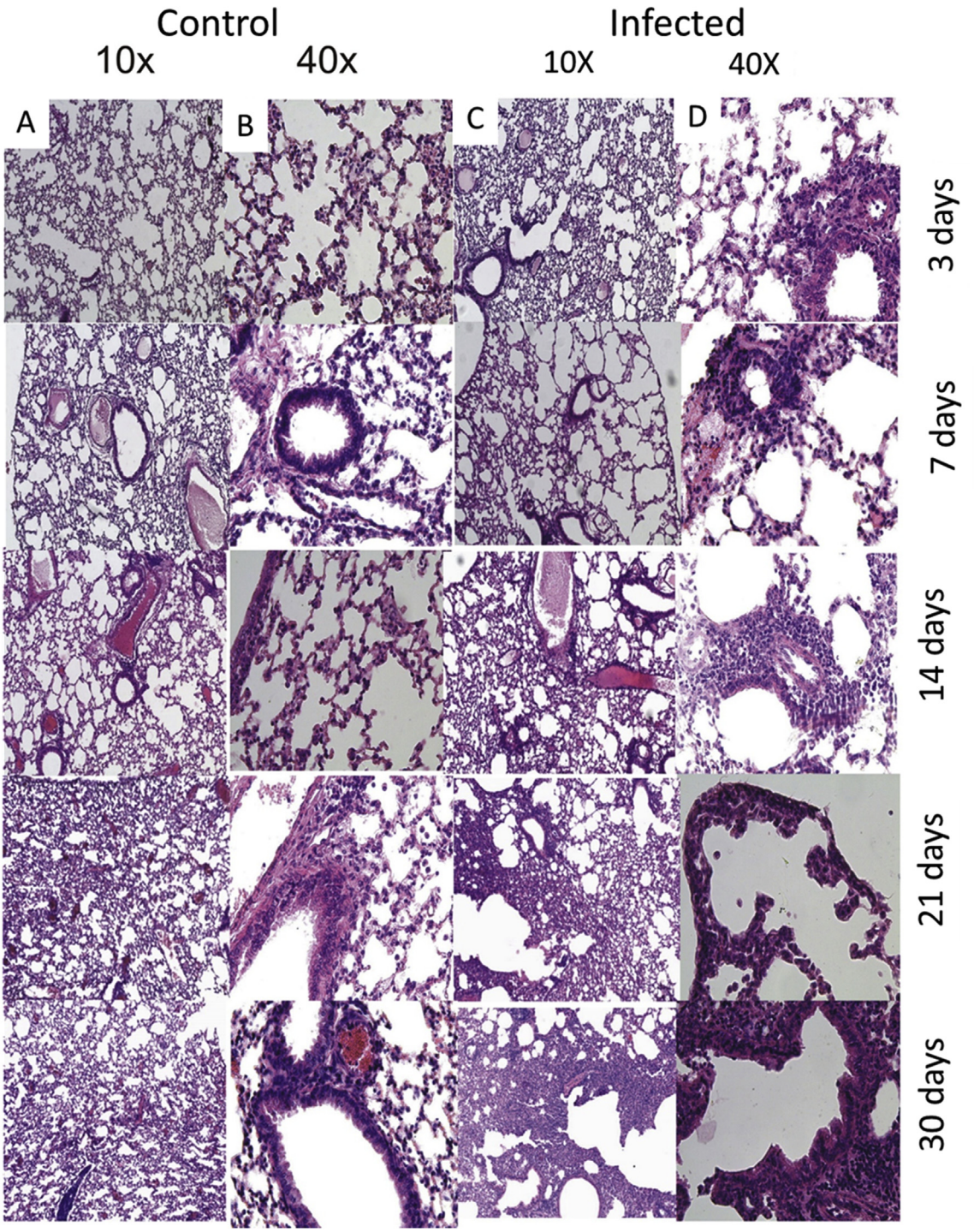

Fig. 2. Hematoxylin-Eosin stain of lung control and infected. Columns A and B correspond to lung of control mice, while columns C and D are from infected lung. As the infection time progress, PMN infiltration is observed. Also, the structure of the lung change. The alveoli fused, and fibrosis process begun (Infected: 14, 21 and 30 days).

in infected mice after 3 and 7 days of infection showed foci of mild inflammatory infiltration around structures of the respiratory tree and in the pulmonary stroma with the presence of 85% of macrophages (M), 10% of lymphocytes (L) and 5% of PMN; polymorphonuclear leukocytes (PMN). The lungs of control mice showed normal distribution of inflammatory cells, 95% of macrophages and 5% of PMN without histological changes.

3.3. Histological analysis

In order to study the impact of *H. pylori* infection on the lung, histological analysis was realized using Hematoxylin-Eosin, Masson's Trichromic and Periodic Acid from Schifft stain. The lungs fixed, sectioned and stained were analysed to evidence injury in tissue of control and infected mice at each infection time.

Hematoxylin-Eosin staining of the lung tissue at 3 days post-infection showed the presence of PMN infiltration around the bronchial tree.

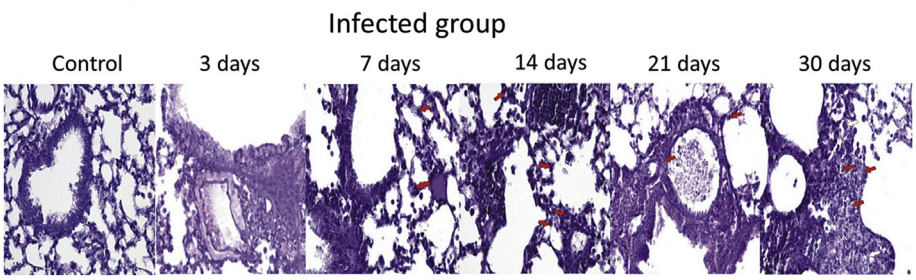

Fig. 3. PAS stain. The picture shows the increased of macrophages during the time of infection. Between days 3 and 14, there is an increase in the same.

PMN infiltration is maintained at 7 days in which the presence of fused alveoli is also observed. The evolution of the damage is evidenced by an increase in infiltration at 14 days coinciding with the beginning of the fibrosis process. The presence of numerous non-functional spaces is observed at 21 days of infection, whereas at 30 days lung tissue shows advanced fibrosis that impacts lung function (Fig. 2).

PAS staining showed a marked presence of macrophages at 3 and 14 days, with an increased during the time of infection. Also, iNOS and IL-8 increased with lung damage indicating an increase of ROS levels of nitrogen in lung tissue (Fig. 3).

Masson's Trichromic staining allows visualization of the connective tissue, which is clearly blue and is mainly present around the respiratory tree (Fig. 4). Analysis of staining in the lung tissue after infection showed an increase in the development of connective tissue in the pulmonary stroma at 3 and 7 days post-infection. At 14 days, the presence of collagen increased considerably, with an evident pulmonary fibrosis at 21 and 30 days post infection, which would compromise the correct functioning of the organ.

3.4. Gene expression analysis

Kinetics was examined of TNF-α, iNOS, IL-1β, IL-8, IL-17, IL-10, IL-4, MMP-9, CCT, I-CAM1 and V-CAM1 mRNA expression, at various time points in response to the orotracheal infection. Kinetic profiles of cytokine gene expression showed heterogeneity over the study period.

As shown in Figs. 5–6, the basal expression of both inflammatory and endothelial dysfunction markers was observed at 3 days post-infection except for IL-1β, which showed an increased at 3 days with a peak on 21 day after infection (Fig. 5B).

TNF-α and IL-17 mRNA expression in the lung of infected mice showed an increased at 7 and 14 days after infection that decreases slightly on day 21 (Figs. 5A and 6B). iNOS and IL-8 showed an increased at 7 and 14 days after infection respectively, while IL-8 has a peak at 21 days (Fig. 5A and B).

Anti-inflammatory IL-4 gene expression profiles showed an increased at 7 days of infection while IL-10 reached peak levels at 14 days (Fig. 5C).

Phosphocholine cytidyltransferase (CCT), the limiting enzyme for the synthesis of phosphatidylcholine, increases its expression from day 14, reaching maximum value at 21 days, while the MMP-9 showed an increased at 7 days with a peak level at 21 day of infection (Fig. 6B).

Finally, the endothelial dysfunction markers, I-CAM1 and V-CAM1 reached maximum levels at 7 days after infection and maintain similar values until day 21 (Fig. 6A).

3.5. Lipid hydroperoxides in lung

Lipid hydroperoxides are related to oxidative stress development in lung. TBARS levels were measured as indicators of lipid peroxidation. At days 3, 7 and 21 after infection, they showed an increase of the infected group in comparison with the corresponding non-infected group. No significant differences were observed at 14 days (Fig. 7).

3.6. Catalase (CAT)

Activity of catalase (CAT) was measured in different times of infection. It was observed an increase in the infected group at days 3, 7 and 21 post infection in comparison to the respective control group. In days 14 no difference was observed between them (Fig. 8).

4. Discussion

The stomach is the natural niche of the *H. pylori*, however in the past few years, extragastric disorders has been associated with infection as: respiratory disease like chronic obstructive pulmonary disease (COPD), bronchiectasis, asthma, lung cancer, chronic bronchitis. In the previously mentioned lung pathologies seroprevalence was seen [24,25]. The present study is the first in evaluate the effect of lung *H. pylori* infection using an animal model which lacks both the vomiting reflex and gastric reflux.

The mechanisms that relate the infection to the development of respiratory diseases it is not defined yet [26]. proposes two theories that would explain: i) the immune response induced by *H. pylori* and the chronic release of gastrointestinal peptides (gastrin, somatostatin) and proinflammatory cytokines, including interleukin IL-1, IL-8 and TNF-α from the gastric mucosa which leads to a systemic effect. ii) A cross molecular mimicry between bacterial and host antigens exists in *H. pylori*-infected patients. Therefore, a pathogenic role of *H. pylori* in diseases may be due to abnormal activation of inflammatory mediators and/or induction of autoimmunity. iii) The aspiration or inhalation of the bacterial in the airways causing a direct damage and chronic airway inflammation [24,27]. Consequently, the possible mechanisms of *H. pylori* infections in the pathogenesis of the majority of extragastric diseases include chronic, local or systemic inflammation and the initiation of autoimmune responses [26].

All available data on *H. pylori* infection in the lungs are based on epidemiological cross-sectional or case-control studies which there are some discrepancies, likely due to the different patient characteristics and diversity of the methods used to detect the microorganism. Almost, several studies have been conducted to demonstrate the association between *H. pylori* and respiratory diseases and to understand the pathogenesis of these diseases [28] hypothesize that the gastric infection of *H. pylori* initiates a systemic immune response that has an impact on the pulmonary in susceptible patients.

[29] Carry out a study to understand the effect of gastric *H. pylori* colonization on local and systemic immune responses. Histological evaluation of the mice's stomach showed corpus-dominant inflammation with mixed mononuclear and neutrophilic infiltrates around the gastric glands. Similarly, in the present study the lung samples showed PMN infiltration around the bronchial tree. Infiltration became evident at 3 days post-infection. Also, the authors observed an increased infiltration with non-functional spaces generation over the course of the infection. According to this, it has been observed that the pathogenesis of some diseases of the upper respiratory system such as otitis and sinusitis showed behaviour similar to the pathogenesis of *H. pylori* gastritis, in which there is an inflammatory response [30].

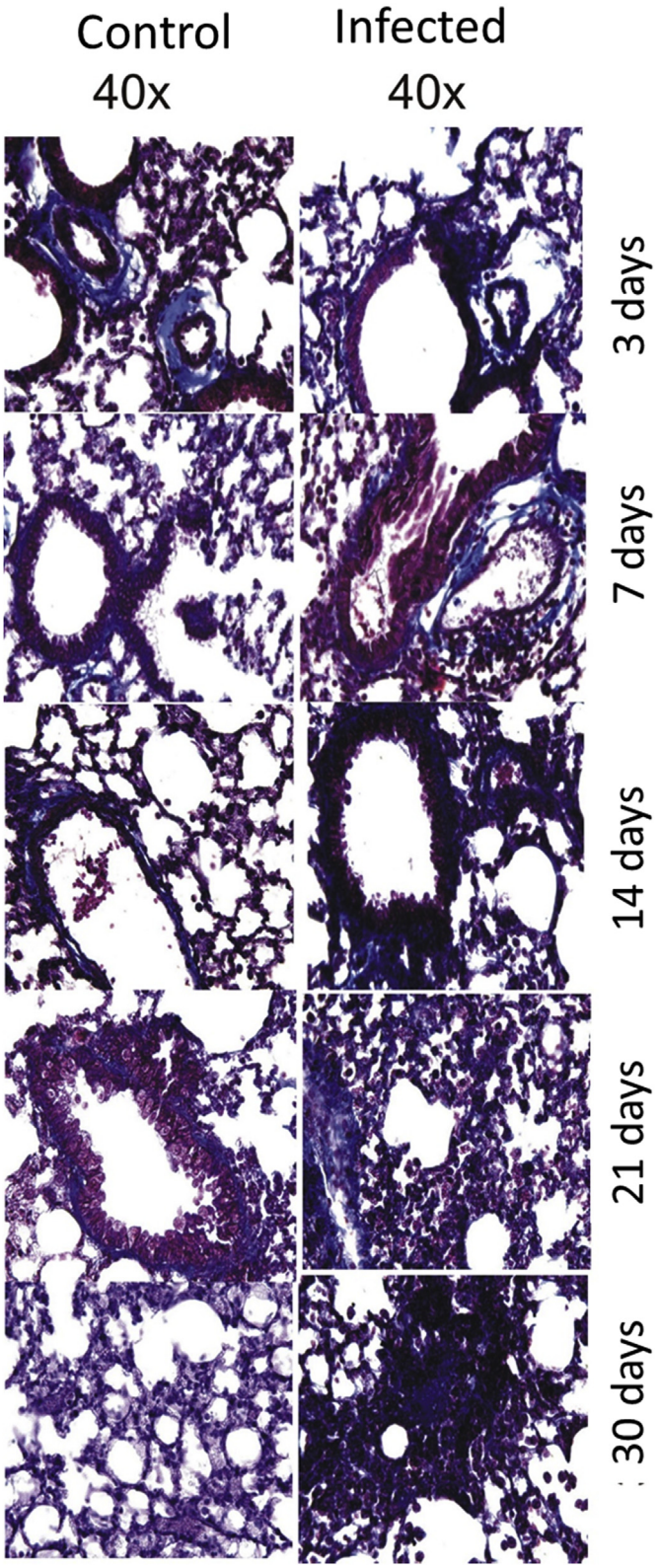

Fig. 4. Masson's Trichromic stain. The connective tissue increases the development in 3 and 7 days after infection. The collagen is considerable at the last days of infection.

On the other hand, we demonstrate that once lung infection with *H. pylori* has occurred, the microorganism colonizes the lung tissue from which it can recover until the seventh day post infection (Fig. 1A and B). We attribute that *H. pylori* cannot be recovery by culture due to a decrease in the bacterial load during the process of lung tissue atrophy observed at 21 and 30 days after infection. Also, the atrophy observed in lung creates a hostile environment for *H. pylori*, and thus it is likely that the organisms were lost after the development of atrophy.

According to this, the molecular detection of *H. pylori* at 21 days after infection only showed a faint band while not amplification of 16S rRNA gene was observed at 30 days. Similar results were obtained by Ref. [31] for detection of *H. pylori* in gastric biopsies using immunohistochemical stain in which the authors did no detected organisms in gastric mucosa with chronic active inflammation. In this sense [32], propose that prolonged atrophy causes the spontaneous disappearance of *H. pylori* from the gastric mucosa and a fall in the antibody titer.

The inflammatory response is mediated by the release of chemokines, cytokines, interferon and enzymes such as metalloproteinases (MMPs). Additionally, the immune cells are the mediators of inflammation to ward off invading pathogens [33] [34]. demonstrate that IL-1β is sufficient to induce lung inflammation, enlargement of distal airspaces, mucus metaplasia, and airway thickening and fibrosis in the adult mouse. Besides, IL-1β enhanced the production of matrix metalloproteases MMP-9 and MMP-12. Consistent with these results, in our experimental model MMP-9 increased (Fig. 6B) after the increased of IL-1β. Both in healthy tissue and tissue in pathological processes express MMPs, a zinc-dependent proteinase whose function are degradation of extracellular matrix and tissue remodeling, playing a key role in the pulmonary inflammation [35]. MMP-9, an elastolytic endopeptidase, produced by active macrophages, an inflammatory cell, from the lung, play a role in the development of pulmonary emphysema by degradation of alveolar wall [36]. Malik et al. [53] observed five days after infection by zymography an increase of MMP-9, in mice's lung, after infection with *Francisella tularensis*. Our results showed peaks of MMP-9 expression at 7 and 21 days, after infection (Fig. 6B).

Malondialdehyde (MDA) and H_2O_2 have been recognized as an important target in the oxidative process, and previous studies have shown that the elevation of oxidative stress indicators is related to heart injury [37]. In our experimental model, *H. pylori* increased antioxidant enzymes catalase (CAT) activity, and improved oxidative production MDA and H_2O_2 level to balance the oxidation and anti-oxidation systems in the lung. In addition, the stimulation of IL-1β and TNF-α causes proliferation of fibroblasts and production of metabolites (ROS and nitrogen species). Reactive oxygen species (ROS), and reactive nitrogen species (such as NO), may also contribute to tissue damage mediated by activated macrophages [38]. At day 3, 7 and 21 post-infection TBARS levels increased, in infected group. In contrast, at day 14, the concentration of TBARS wasn't increased significantly between the groups (Fig. 7). These results provide additional evidence for the concept that oxidative stress is an important effect of *H. pylori* infection, in lung. To compare the lung oxidative status of infected mice, an analysis of CAT activity was undertaken. We detected an increased in CAT at 3, 7 and 21 days after *H. pylori* infection; these increments are associated at the time that TBARS increased (Fig. 8).

H. pylori´s LPS and cytokines through activation of different signaling pathways can induce the expression of nitric oxide synthase inducible (iNOS). The resulting product, NO, has anti-bacteria and antivirus properties, and the excess is involved in inflammatory an infectious disorder [39]. Our results show an increase of mRNA, reaching a peak at 14 days after infection, with a decreased in the next days. Similar results were obtained by Ref. [40] in mice's lungs infected with *Mycobacterium tuberculosis*. In addition, it is quite possible that secondary metabolites of nitrites, on the other function as potent chemotaxis for polymorphonuclear neutrophils and macrophages [41].

Several authors showed that IL-17 A acts in synergy with IL-1β and TNF-α to drive the inflammatory environment; also stimulate human epithelial cells to induce IL-8 cytokine [54]. After the 7 days post-infection, IL-17 was overexpressed, this agree with results from other

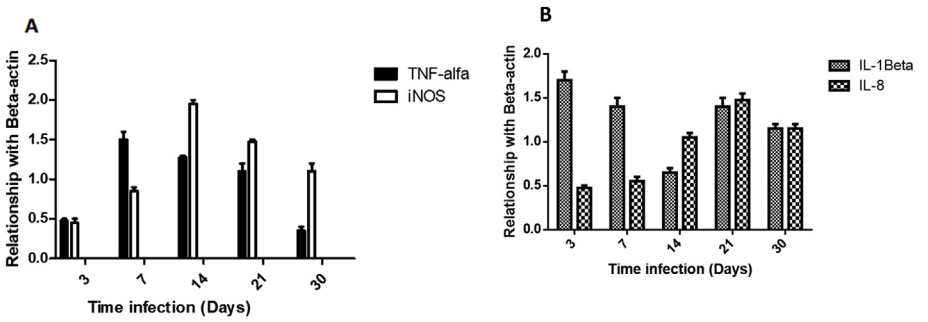

Fig. 5. Analysis of gene expression. **A)** An increase of TNF-α was observed from day 7 to day 21 after infection, while iNOS showed a higher expression at day 14. **B)** IL-1β have high levels of expression during the day 3 and day 21. IL-8 showed a peak in day 21. **C)** Anti-inflammatory cytokines IL-4 and IL-10 have a peak at day 7 and day 21, also IL-10 have a maximum peak at day 14.

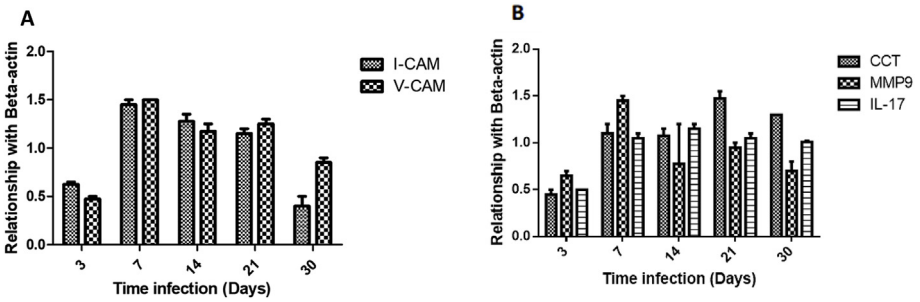

Fig. 6. A) An increase of both endothelial adhesion molecules I-CAM1 and V-CAM1 was observed from day 7 to day 21. **B)** CIT showed a higher expression at day 21, while IL-17 had a constant expression over time. MMP-9 showed a peak at day 7, after that it was decreasing.

authors that showed an increase of this interleukin in patients infected with *H. pylori* in gastric mucosa [42]. In addition, IL-17 is associated with antimicrobial responses and control of bacterial colonization in several animal models [43]. In this study, as expected, the microorganism it was not recovered from lung tissue at 14 days after infection, according to the higher values observed by IL-17, among days 7–30 after infection. In this sense, several authors propose that the strong inflammatory responses at mucosal gastric level lead to eradication of *H. pylori* [44].

IL-4 is a cytokine that promotes and regulated immune response, some authors demonstrate that secretion of IL-17 is downregulated by IL-4 [45,46]. However, in this study IL-17 was overexpressed from 7 to 30 days, after infection. Also, IL-4 increased the expression of IL-10 [45]. We found a peak of IL-10 after increased of IL-4. High levels of IL-10 may mask proinflammatory effects of TNF-α [47]. In our study the increase level of IL-10 coincided with low level of TNF-α. Respect to TNF-α, it has a peak at 7 days after infection and then the cytokine decreased. Similar results were observed with *M. tuberculosis* at 3 weeks (21 days) after infection [40,48]. The initial steps of endothelium/leucocyte interactions are considered to involve selectins and I-CAM, V-CAM. These are crucial for leucocytes adhesion and migration into the sub-endothelium. Additionally, TNF-α increased the expression of intracellular adhesion molecule-1 (I-CAM1), that mediates the transmigration of enrolled leucocytes into the surrounding tissue. At seven days, it was noted that I-CAM and V-CAM was remarkably increased in the lung of infected mice. Besides, both endothelial adhesive molecules remain elevated until day 21. So, the elevation of cell adhesive molecules is related to higher morbidity and these cytokines are considered as reliable biomarkers of endothelial activation.

Under these conditions (increase inflammatory cytokines and growth factor as IL-1β, TNF-α, IL-17 and IL-8) the interaction among activated macrophages, infiltrated neutrophils, alveolar cells, and vascular endothelial cells in alveolar space potentiate moderate to severe inflammation, amplifying a cascade of inflammatory reactions and modification of the surfactant synthesis (Fig. 5A and B and 6B) [49]. The effect of altered surfactant phospholipid metabolism and its distinct influence on the pathogenesis of lung pathology is often underappreciated because attention is frequently focused on the primary source, the type 2 pneumocyte (AT2). Phosphocholine cytidyltransferase (CCT) considered a marker of damage of pulmonary stroma that lead to alteration of surfactant synthesis showed higher values at seven days after infection. CCT showed a high level in the last days of infection that compromises the synthesis of pulmonary surfactant major component, affecting organ function. These results are according to lung tissue damage observed by histological analysis, in other pathological situation [52,49]. Accordingly, altered surfactant homeostasis is commonly considered an inevitable consequence secondary to AT2 cell dysregulation and injury.

Otherwise, the infiltration of inflammatory cells within the gastric mucosa is a common factor in *H. pylori* infection, and the degree of mucosal damage correlates with PMN infiltration [11]. Hematoxylin-eosin-stained lung sections obtained from *H. pylori* infected mice, at day

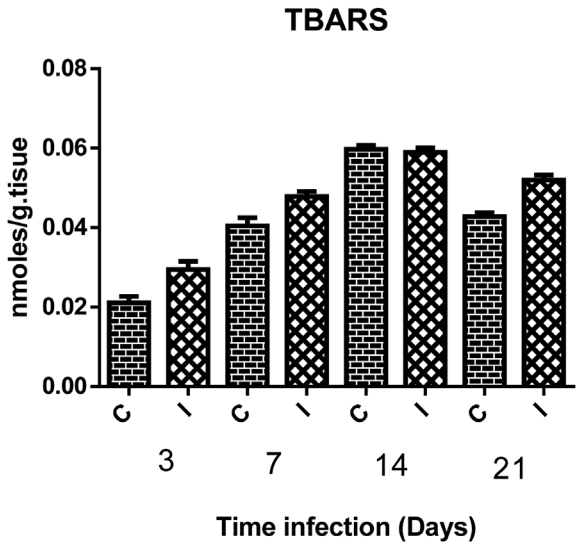

Fig. 7. Oxidative stress in the lung. Thiobarbituric acid-reactive substances (TBARS) in lung of control (C) group and infected (I) group with *H. pylori*. Data are means ± SEM, n = 4. Representative results from three independent experiments are shown. TBARS were measured as indicators of lipid peroxidation. No significant differences were detected between Control and infected group at day 14. The concentration of TBARS in infected mice increased significantly between 3 and 7 days compared with corresponding non infected groups (*p < 0.01, **p < 0.001). Also, on day 21 TBARS levels were significantly higher in lung of infected mice (#p < 0.01) compared to Control mice.

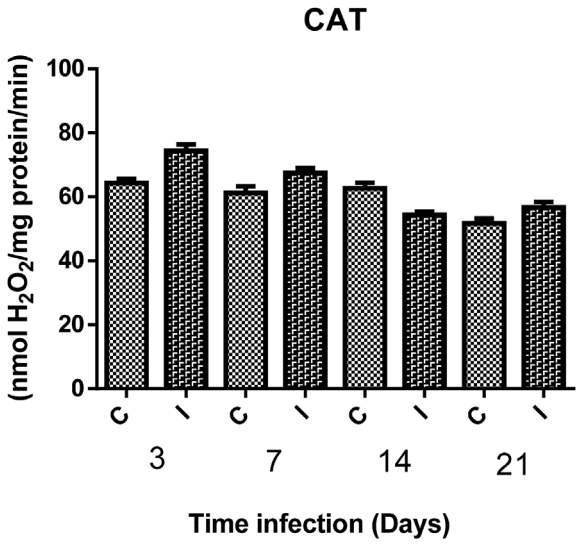

Fig. 8. Effects of different infection period (7, 14, 21 and 30 days) with *H. pylori* in Catalase enzyme. An increased was observed at 3, 7 and 21 days post-infection. There was no significant difference in day 14 in comparison with control group.

3 after infection revealed foci of mild inflammatory infiltration of bronchioles and adjacent alveoli. The lung from the non-infected animals did not show such histopathological features. The interstitial space contained a large number of blood cells, predominantly polymorphonuclear inflammatory cells, when compared to control mice.(Fig. 2). Neutrophils and activated macrophages also degrade surfactant lipids suggesting that both cell types may contribute to the alterations in the lipid surfactant [50]. At 7 days post-infection, infiltration of phagocytic cells, revealed fragmentation of the alveolar septa, focal interstitial proliferation, and mononuclear inflammatory cell infiltration. Likewise, IL-17 pathway may destroy the tissue by inducing MMP production [51]. At day 21 and 30 after infection more significant changes in lung parenchyma were observed in both groups compared with infected animals at day 3 and 7. At 21 day Masson's trichrome stain reveals increased collagen on alveolar walls of lung infected mice compared with controls, and specially increased collagen, at 30 days (Fig. 4). Mucus metaplasia is commonly associated with chronic inflammatory lung diseases. From the 7 day, PAS staining revealed mucus metaplasia in the lungs of infected mice compared with control (Fig. 3).

Our results suggest that the pathogenic mechanism of *H. pylori* in the lung is strongly evidenced with pulmonary tissue damage associated with increased expression of inflammation mediators and markers of endothelial dysfunction. In addition, this knowledge is crucial for understanding how mononuclear inflammatory cell and phagocytic cells participate in antimicrobial host defense and inflammatory tissue damage which may also point to possible future targets of the pharmacological therapy.

5. In conclusion

The impact of *Helicobacter pylori* infection on the respiratory system represents a field with inconclusive data and many pending questions.

This is the first work that shows the effect of lung *H. pylori* infection using a mouse animal model. Results exhibited direct evidence and revealed a bacterial potential pathogenic role in the tissue injure, the expression of cytokines and endothelial dysfunction markers. Considering the importance and prevalence of respiratory system diseases; these work is an important contribution in the study of the possible link between *H. pylori* and pulmonary pathology.

Acknowledgments

Financial support was provided by UNSL (PROICO 2-4118 and PROICO 2-2317). Authors appreciate language manuscript revision by Dra. Ciminari ME.

References

[1] L.E. Wroblewski, rm Peek, K.T. Wilson, *Helicobacter pylori* and gastric cancer: factors that modulate disease risk, Clin. Microbiol. Rev. 23 (4) (2010) 713–739.
[2] G. Posselt, S. Backert, S. Wessler, The functional interplay of *Helicobacter pylori* factors with gastric epithelial cells induces a multi-step process in pathogenesis, Cell Commun. Signal. 11 (2013) 7 2013.
[3] Y. Yamaoka, Mechanisms of disease: *Helicobacter pylori* virulence factors, Nat. Rev. Gastroenterol. Hepatol. 7 (2010) 629–641.
[4] H.K. Takahiro, H. Naoki, S. Takashi, A. Yoh, Y. Taku, M. Takeshi, M. Masato, I. Tadakatsu, M. Shigeru, S. Yoshiki, M. Masaaki, K. Atsushi, Y.T. Keiko, O. Meinoshin, K. Tadamitsu, K. Issei, S. Mikiyasu, S. Yasushi, N. Yoshikazu, Interleukin-6/interleukin-21 signalling axis is critical in the pathogenesis of pulmonary arterial hypertension, PNAS Plus (2015) 2677–2686.
[5] R.A. Karttunen, T.J. Karttunen, M.M. Yousfi, Expression of mRNA for interferon-gamma, interleukin-10, and interleukin-12 (p40) in normal gastric mucosa and in mucosa infected with *Helicobacter pylori*, Scand. J. Gastroenterol. 32 (1997) 22–27.
[6] R. Rad, A. Dossumbekova, B. Neu, R. Lang, S. Bauer, D. Saur, M. Gerhard, C. Prinz, Cytokine gene polymorphisms influence mucosal cytokine expression, gastric inflammation, and host specific colonisation during *Helicobacter pylori* infection, Gut 53 (2004) 1082–1089.
[7] Y. Shi, X.F. Liu, Y. Zhuang, J.Y. Zhang, T. Lius, Z. Yin, C. Wu, X.H. Mao, K.R. Jia, F.J. Wang, H. Gou, R.A. Flavell, Z. Zhao, K.Y. Liu, B. Xiao, Y. Guo, W.J. Zhang, W.Y. Zhou, G. Gou, Q.M. Zou, *Helicobacter pylori*-Induced Th17 responses modulate Th1 cell response, benefit bacterial growth, and contribute to pathology in mice, J. Immunol. 184 (2010) 5121–5129.
[8] S.L. Gaffen, An overview of IL-17 function and signalling, Cytokine 43 (2008) 402–407.
[9] J. Ji, J. Huan Dou, X. Li, Y. Song, K. Li, E. Li, R. Tan, Y. Hou, Novel benzenediamine derivative FC99 ameliorates zymosan-induced arthritis by inhibiting RORγt expression and Th17 cell differentiation, Acta Biochim. Biophys. Sin. 46 (2014) 829–836.
[10] S. Assis, C. Rodrigues Marques, T. Magalhaes Silva, R. Santos Costa, N.M. Alcantara-Neves, M. Lima Barreto, K.C. Barnes, C.A. Figueiredo, IL10 single nucleotide polymorphisms are related to up regulation of constitutive IL-10 production and susceptibility to *Helicobacter pylori* infection, Helicobacter 19 (2014) 168–173.
[11] M.M. D'Elios, L.P. Andersen, *Helicobacter pylori* inflammation, immunity, and vaccines, Helicobacter 12 (1) (2007) 15–19.
[12] PCh Konturex, T. Brzozowski, S.J. Konturex, J. Stachura, E. Karczewska, R. Pajdo,

P. Ghiara, E.G. Hahn, Mouse model of *Helicobacter pylori* infection: studies of gastric functions and ulcer healing, Aliment. Pharmacol. Ther. 13 (1999) 333–346.
[13] N. Mori, H. Sato, T. Hayashibara, M. Senba, R. Geleziunas, A. Wada, T. Hirayama, N. Yamamoto, *Helicobacter pylori* induces matrix metalloproteinase-9 through activation of nuclear factor kappa B, Gastroenterology 124 (2003) 983–992.
[14] Y. Zhou, G. Guo, Z. Quan-Ming, L. Kai-Yun, X. Bin, Y. Guo, Wei-Jun, W. Feng-Jun, G. Hong, R.A. Flavell, Z. Zhuo, Y. Zhinan, C. Wu, M. Xu-Hu, J. Ke-Ran, S. Yun, L. Xiao-Fei, Z. Yuan, T. Jin-Yu Zhang, Helicobacter pylori-induced Th17 responses modulate Th1 cell responses, benefit bacterial growth, and contribute to pathology in mice, J. Immunol. 184 (2010) 5121–5129.
[15] M. Malik, C.S. Bakshi, K. McCabe, S.V. Catlett, A. Shas, R. Singh, P.L. Jackson, A. Gaggar, D.W. Metzger, J.A. Melendez, J.E. Blalock, T.J. Sellati, Matrix metalloproteinase 9 activity enhances host susceptibility to pulmonary infection with type A and B strains of *Francisella tularensis*, J. Immunol. 178 (2) (2007) 1013–1020.
[16] E. Goni, F. Franceschi, *Helicobacter pylori* and Extragastric Diseases Helicobacter vol. 21, (2016), pp. 45–48.
[17] N. Figura, F. Franceschi, A. Santucci, G. Bernardini, G. Gasbarrini, A. Gasbarrini, Extragastric manifestations if *Helicobacter pylori* infection, Helicobacter 15 (1) (2010) 60–68.
[18] B. Deng, Y. Li, Y. Zhang, L. Bai, P. Yang, *Helicobacter pylori* infection and lung cancer: a reviews of an emerging hypothesis, Carcinogenesis 34 (6) (2013) 1189–1195.
[19] M. Samareh-Fekri, S.M. Hashemi Bajgani, A. Shafahi, M. Asadi-Zarandi, H. Mollaie, A.J. Paghalhe, Detection of *Helicobacter pylori* in the bronchoalveolar lavage of patients with lung cancer using real-time PCR, Jundishapur J. Microbiol. 9 (11) (2016) 1–6.
[20] F. Franceschi, A. Tortora, G. Gasbarrini, A. Gasbarrini, *Helicobacter pylori* and extragastric diseases, Helicobacter 19 (1) (2014) 52–58.
[21] S. Nakashima, T. Kakugawa, H. Yura, M. Tomonaga, T. Harada, A. Hara, S. Hara, M. Nakano, E. Yamasaki, N. Sakamoto, Y. Ishimatsu, H. Isomoto, B.R. Gochuico, A.F. Suffredini, H. Mukae, H. Kurazono, T. Hirayama, J. Moss, S. Kohno, Identification *of Helicobacter pylori* VacA in human lung and its effects on lung cells, Biochem. Biophys. Res. Commun. 460 (3) (2015) 721–726.
[22] A.S. Awaad, A.M. Alafeefy, F.A.S. Alasmary, R.M. El-Meligy, M.E. Zain, S.I. Alqasoumi, Novel essential amino acid-sulfanilamide hybrid as safe anti-ulcerogenic agent with anti-*Helicobacter pylori* activity, Saudi Pharmaceut. J. 25 (2017) 967–971.
[23] J.G. Gutierrez, S.R. Valdez, S. Di Genaro, N.N. Gómez, Interleukin-12p40 contributes to protection against lung injury after oral *Yersinia enterocolitica* infection, Inflamm. Res. 57 (2007) 504–511.
[24] M.V. Malfertheiner, A. Kandulski, J. Schreiber, P. Malfertheiner, *Helicobacter pylori* infection and the respiratory system: a systematic review of the literature, Digestion 84 (3) (2011) 212–220.
[25] N.O. Shams-Hosseini, S.A. Mousavi, M. Kadivar, E. Ahmadipour, R. Yazdani, V. Moradians, *Helicobacter pylori* in patients suffering from pulmonary disease, Tanaffos 10 (1) (2011) 31–36.
[26] M. Chmiela, Z. Karwowska, W. Gonciarz, B. Allushi, P. Stączek, Host pathogen interactions in *Helicobacter pylori* related gastric cancer, World J. Gastroenterol. 23 (9) (2017) 1521–1540.
[27] A. Roussos, N. Philippou, G.J. Mantzaris, K.I. Gourgoulianis, Respiratory diseases and *Helicobacter pylori* infection: is there a link? Respiration 73 (5) (2006) 708–714.
[28] M. Kreuter, D. Kirsten, T. Bahmer, R. Penzel, M. Claussen, S. Ehlers-Tenenbaum, T. Muley, K. Palmowski, M. Eichinger, M. Leider, F.J. Herth, K.F. Rabe, I. Bittmann, A. Warth, Screening for Helicobacter pylori in Idiopathic Pulmonary Fibrosis Lung Biopsies Respiration vol. 91, (2006), pp. 3–8.
[29] S. Kienesberger, L.M. Cox, A. Livanos, X.S. Zhang, J. Chung, G.I. Perez-Perez, G. Gorkiewicz, E.L. Zechner, M.J. Blaser, Gastric *Helicobacter pylori* infection affects local and distant microbial populations and host responses, Cell Res. 14 (6) (2016) 1395–1407.
[30] H. Kurtaran, M.E. Uyar, B. Kasapoglu, C. Turkay, T. Yilmaz, A. Akcay, M. Kanbay, Role of *Helicobacter pylori* in pathogenesis of upper respiratory system diseases, J. Natl. Med. Assoc. 100 (10) (2008) 1224–1230.
[31] A. Sonnenberg, R.H. Lash, R.M. Genta, A National Study of Helicobacter pylori infection in gastric biopsy specimens, Gastroenterology 139 (2010) 1894–1901.
[32] W.E. Karnes, I.M. Samloff Jr., M. Siurala, Positive serum antibody and negative tissue staining for Helicobacter pylori in subjects with atrophic body gastritis, Gastroenterology 101 (1991) 167–174.
[33] S.K. Pachathundikandi, S. Brandt, J. Madassery, S. Backert, Induction of TLR-2 and TLR-5 expression by *Helicobacter pylori* switches cagPAI-dependent signalling leading to the secretion of IL-8 and TNF-α, PLoS One 6 (5) (2011) e19614.
[34] U. Lappalainen, J.A. Whitsett, S.E. Wert, J.W. Tichelaar, K. Bry, Interleukin-1beta causes pulmonary inflammation, emphysema, and airway remodeling in the adult murine lung, Am. J. Respir. Cell Mol. Biol. 32 (4) (2005) 311–318.
[35] N. Kondo, T. Temma, K. Aita, S. Shimochi, K. Koshino, M. Senda, H. Iida, Development of matrix metalloproteinase-targeted probes for lung inflammation detection with positron emission tomography, Sci. Rep. 8 (2018) 1347.
[36] Y. Li, Y. Lu, Z. Zhao, J. Wang, J. Li, W. Wang, S. Li, L. Song, Relationships of MMP-9 and TIMP-1 proteins with chronic obstructive pulmonary disease risk: a systematic review and meta-analysis, J. Res. Med. Sci. 21 (2016) 12.
[37] L. Xianchu, Z. Lan, L. Ming, M. Yanzhi, Protective effects of rutin on lipopolysaccharide-induced heart injury in mice, J. Toxicol. Sci. 43 (5) (2018) 329–337.
[38] D.L. Laskin, K.J. Pendino, Macrophages and inflammatory mediators in tissue injury, A nn. Rev. Pharmacol. Toxicol. 35 (1995) 655–677.
[39] D. Dang, C. Zhang, R. Zhang, W. Wu, S. Chen, J. Ren, P. Zhang, G. Zhou, D. Feng, T. Sun, S. Li, Q. Liu, M. Li, Y. Xi, Y. Jin, G. Duan, Involvement of inducible nitric oxide synthase and mitochondrial dysfunction in the pathogenesis of enterovirus 71 infection, Oncotarget 8 (46) (2017) 81014–81026.
[40] D. Aguilar, M. Hanekom, D. Mata, N.C. Gey van Pittius, P.D. van Helden, R.M. Warren, R. Hernandez-Pando, *Mycobacterium tuberculosis* strains with the Beijing genotype demonstrate variability in virulence associated with transmission, Tuberculosis 90 (5) (2010) 319–325.
[41] N.N. Gómez, R.C. Davicino, V.S. Biaggio, G.A. Bianco, S.M. Alvarez, P. Fischer, L. Masnatta, G.A. Rabinovich, M.S. Gimenez, Overexpression of inducible nitric oxide synthase and cyclooxygenase-2 in rat zinc-deficient lung: involvement of a NF-kappaB dependent pathway, Nitric Oxide 14 (1) (2006) 30–38.
[42] R. Caruso, D. Fina, O.A. Paoluzi, G. Del Vecchio Blanco, C. Stolfi, A. Rizzo, F. Caprioli, M. Sarra, F. Andrei, M.C. Fantini, T.T. MacDonald, F. Pallone, G. Monteleone, IL-23-mediated regulation of IL-17 production in *Helicobacter pylori*-infected gastric mucosa, Eur. J. Immunol. 38 (2) (2008) 470–478.
[43] B.R. Dixon, J.N. Radin, M.B. Piazuelo, D.C. Contreras, H.M. Algood, IL-17a and IL-22 induce expression of antimicrobials in gastrointestinal epithelial cells and may contribute to epithelial cell defense against *Helicobacter pylori*, PLoS One 11 (2) (2016).
[44] H.M. Scott Algood, T.L. Cover, *Helicobacter pylori* persistence: an overview of interactions between *H*, *Pylori* and Host Immune Defenses Clin Microbiol Rev 19 (4) (2006) 597–613.
[45] C.P. Fernandez, F. Afrin, R.A. Flores, W.H. Kim, J. Jeong, Kim, H.S. Lillehoj, W. Min, Identification of duck IL-4 and its inhibitory effect on IL-17A expression in *R. anatipestifer*-stimulated splenic lymphocytes, Mol. Immunol. 95 (2018) 20–29.
[46] E. Guenova, Y. Skabytska, W. Hoetzenecker, G. Weindl, K. Sauer, M. Tham, K.W. Kim, J.H. Park, J.H. Seo, D. Ignatova, A. Cozzio, M.P. Levesque, T. Volz, M. Köberle, S. Kaesler, P. Thomas, R. Mailhammer, K. Ghoreschi, K. Schäkel, B. Amarov, M. Eichner, M. Schaller, R.A. Clark, M. Röcken, T. Biedermann, IL-4 abrogates T(H)17 cell-mediated inflammation by selective silencing of IL-23 in antigen-presenting cells, Proc. Natl. Acad. Sci. U. S. A. 112 (7) (2015) 2163–2168.
[47] K.A. Eaton, M. Mefford, T. Thevenot, The Role of T Cell subsets and cytokines in the pathogenesis of *Helicobacter pylori* gastritis in mice, J. Immunol. 166 (2001) 7456–7461.
[48] I.S. Roh, S. Cho, S.Y. Eum, S.N. Cho, Kinetics of IFN-gamma and TNF-alpha gene expression and their relationship with disease progression after infection with *Mycobacterium tuberculosis* in Guinea pigs, Yonsei Med. J. 54 (3) (2013) 707–714.
[49] V.S. Biaggio, M.V. Pérez Chaca, S.R. Valdéz, N.N. Gómez, M.S. Gimenez, Alteration in the expression of inflammatory parameters as a result of oxidative stress produced by moderate zinc deficiency in rat lung, Exp. Lung Res. 36 (1) (2010) 31–44.
[50] O.A. Quintero, J.R. Wright, Clearance of surfactant lipids by neutrophils and macrophages isolated from the acutely inflamed lung, Am. J. Physiol. 282 (2002) 330–339.
[51] P. Mitchell, C. Germain, P.L. Fiori, W. Khamri, G.R. Foster, S. Ghosh, R.I. Lechler, K.B. Bamford, G. Lombardi, Chronic exposure *to Helicobacter pylori* impairs dendritic cell function and inhibits Th1 development, Infect. Immun. 75 (2007) 810–819.
[52] N.N. Gomez, V.S. Biaggio, E.J. Rozzen, S.M. Alvarez, M.S. Gimenez, Zn-limited diet modifies the expression of the rate-regulatory enzymes involved in phosphatidylcholine and cholesterol synthesis, Br. J. Nutr. 96 (6) (2006) 1038–1046.
[53] M. Malik, C.S. Bakshi, K. McCabe, S.V. Catlett, A. Shas, R. Singh, P.L. Jackson, A. Gaggar, D.W. Metzger, J.A. Melendez, J.E. Blalock, T.J. Sellati, Matrix metalloproteinase 9 activity enhances host susceptibility to pulmonary infection with type A and B strains of *Francisella tularensis*, J. Immunol. 178 (2) (2007) 1013–1020.
[54] J. Ji, J. Huan Dou, X. Li, Y. Song, K. Li, E. Li, R. Tan, Y. Hou, Novel benzenediamine derivative FC99 ameliorates zymosan-induced arthritis by inhibiting RORγt expression and Th17 cell differentiation, Acta Biochim. Biophys. Sin. 46 (2014) 829–836.